

## Surface excitons in ZnO crystals

This article has been downloaded from IOPscience. Please scroll down to see the full text article.

1989 J. Phys.: Condens. Matter 1 847

(<http://iopscience.iop.org/0953-8984/1/5/002>)

View [the table of contents for this issue](#), or go to the [journal homepage](#) for more

Download details:

IP Address: 171.66.16.90

The article was downloaded on 10/05/2010 at 17:06

Please note that [terms and conditions apply](#).

## Surface excitons in ZnO crystals

V M Harutunian, H L Margarian, V A Melicksetian and J R Panossian  
Yerevan State University, Mravian 1, 375049, Yerevan, Armenian SSR, USSR

Received 23 March 1987, in final form 11 August 1987

**Abstract.** The spectra of the photocurrent through a ZnO–electrolyte interface, and the photoconductivity and the photoluminescence of ZnO, together with the direction diagrams for various emission lines, were investigated. The peculiarities observed near the fundamental absorption edge of ZnO were connected with the formation of quasi-two-dimensional and two-dimensional excitons.

### 1. Experiment

The spectral characteristics of photoconductivity (PC), the photocurrent through the interface and the photoluminescence (PL), which depend on both the condition of the surface and the surface potential, were investigated, together with the direction diagrams for various emission lines.

ZnO single crystals were grown by the hydrothermal method [1] and polycrystals were obtained by high-temperature baking [2]. The Ohmic contact was prepared using the indium vacuum deposition technique.

To investigate PC spectra, the well known method of mechanical modulation of luminous flow ( $\nu = 75$  Hz) was used. The photocurrent through the semiconductor–electrolyte interface was obtained in the same way, but in this case the cryostat was replaced by a photo-electrochemical cell. Pt was used as the counter-electrode and 1 N KCl or NaOH was the electrolyte. The photosignal was obtained from the load resistor connected between ZnO and the counter-electrodes.

In order to obtain PL spectra, a nitrogen laser with a 6–8 ns pulse duration and a 3371 Å wavelength was used for the photo-excitation.

#### 1.1. Photoconductivity

The PC spectra of two polycrystalline samples 1 and 2 with  $N_D - N_A$  equal to  $10^{18}$  cm<sup>-3</sup> and  $10^{19}$  cm<sup>-3</sup>, respectively, were obtained in the temperature range 78–300 K. The results are shown in figure 1. A sharp drop in photosensitivity was observed in curves A and B obtained at  $T = 78$  K; this minimum was shifted towards the longer-wavelength region compared with the bulk exciton  $E_0$  (see the upper scale) by 50 meV for sample 1 and by 73 meV for sample 2.

The main minimum widens and shifts toward lower energies with increase in temperature (as does the bulk exciton line [1, 3]) as shown for sample 2 (curves B–D). Note

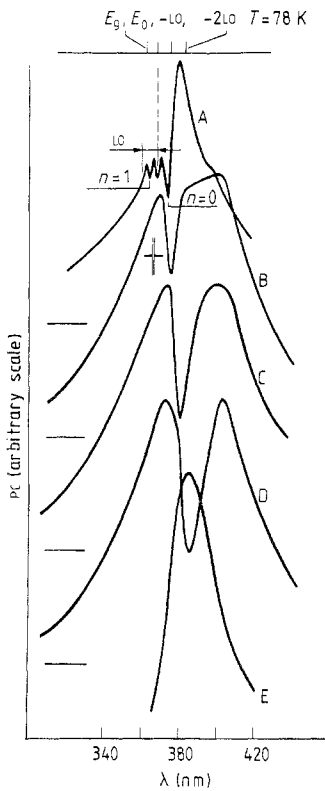


**Figure 1.** PC spectra of two polycrystalline ZnO samples with  $N_D - N_A = 10^{18} \text{ cm}^{-3}$  (curve A) and  $N_D - N_A \approx 10^{19} \text{ cm}^{-3}$  (curves B–D) and one monocrystalline sample (curve E). Curves A and B were obtained at  $T = 80 \text{ K}$ , curve C at  $T = 170 \text{ K}$  and curves D and E at  $T = 300 \text{ K}$ .

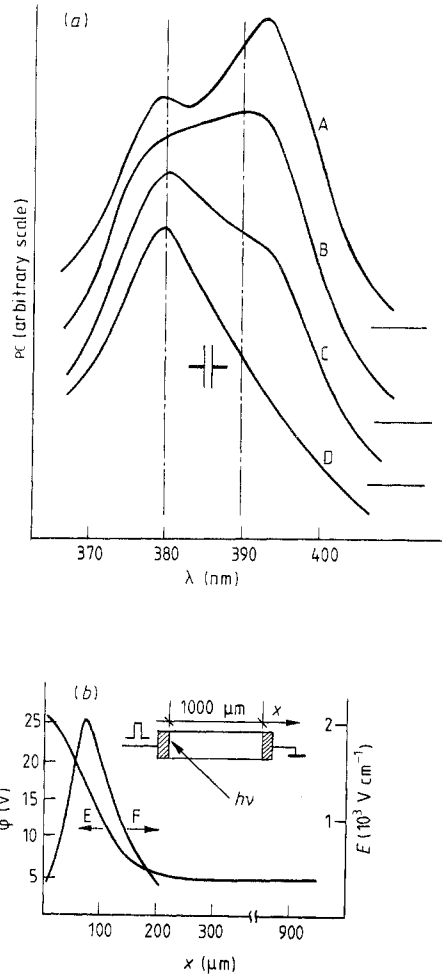


**Figure 2.** (a) Variation in the PC spectra of ZnO single crystals for various  $x$ -values at  $T = 300 \text{ K}$ : curve A,  $x = 300 \mu\text{m}$ ; curve B,  $x = 180 \mu\text{m}$ ; curve C,  $x = 120 \mu\text{m}$ ; curve D,  $x = 50 \mu\text{m}$ . (b) The distributions of the surface potential (curve E) and the field intensity (curve F) in the inter-contact region.

that this line, which depends on the condition of the surface, can appear as a maximum (curve E).

Apart from the main minimum ( $\lambda = 373.9 \text{ nm}$ ) a structure with two minima was observed in the shorter-wavelength region of the PC spectrum (curve A). The first minimum ( $\lambda = 367.8 \text{ nm}$ ) coincided with the bulk exciton line and its spectral position was the same for different samples, whereas the minimum at  $\lambda = 364 \text{ nm}$  changed in step with the main minimum. The difference between the lines at  $\lambda = 373.9 \text{ nm}$  and  $\lambda = 364 \text{ nm}$  is about  $90 \text{ meV}$ , which is much larger than the longitudinal optical (LO) phonon energy ( $71 \text{ meV}$  [3]) in ZnO crystals, while the first-phonon replica of the bulk exciton is observed as a sharp drop in the short-wavelength region of the PC spectrum.

The change in the PC spectra can be obtained not only by mechanical and chemical treatment of the crystal surface but also by varying the surface potential (figure 2). As the contacts deposited on the ZnO surface were non-Ohmic, the distributions of the potential  $\varphi$  and the field strength  $E$  in the inter-contact region with respect to  $x$  are as presented in figure 2(b) (curves E and F, respectively). The PC spectra shown in figure 2(a) indicate the excitation at different points along the  $x$  axis. For large  $x$ , i.e. far from the region where there is a marked change in the surface field intensity (see figure 2(b)), two maxima, one at 380 nm and the other at 392 nm, were observed. Strong quenching of the line at the longer wavelength was observed when the maximum surface potential region was illuminated.

### 1.2. Photocurrent through the semiconductor–electrolyte interface

As is pointed out in § 1.2, the peculiarities obtained in the PC spectra of ZnO crystals in the region of exciton absorption were strongly dependent on the condition of the surface. From this point of view, photo-electrochemical investigations would be suitable for considering such a problem, since one can smoothly vary the value of the surface potential of the semiconductor by applying an external bias between the ZnO crystal and the Pt counter-electrode. A typical spectrum of the photocurrent through the ZnO–electrolyte interface is shown in figure 3 (curve A). The photocurrent due to absorption in both the intrinsic and the impurity regions has been investigated by us previously [4].

The interesting peculiarity in the spectrum is the drop in photosensitivity, which cannot be explained by the overlap of two different lines because of its sharpness and depth. Such peculiarities, which exist in the spectra of both the PC and the interface

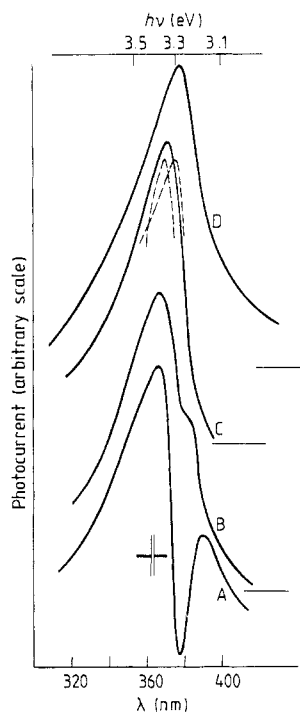


**Figure 3.** Photocurrent spectra of a single-crystal ZnO–electrolyte junction at various external biases  $V_{\text{ex}}$  at  $T = 300$  K: curve A,  $V_{\text{ex}} = -0.5$  V; curve B,  $V_{\text{ex}} = -0.4$  V; curve C,  $V_{\text{ex}} = 0$  V; curve D,  $V_{\text{ex}} = 2.5$  V.

photocurrent, are explained by exciton absorption which does not normally lead to the formation of free-charge carriers. Nevertheless the energy position of the photosensitivity drop does not correspond to the known value of the bulk exciton binding energy for ZnO. When the sample is illuminated by polarised light ( $E \perp C$  and  $E \parallel C$ ) a shift of 0.04 eV in the photocurrent maximum was observed (which is in good agreement with the magnitude of the splitting due to the presence of the hexagonal field), indicating the exciton nature of these lines (curve C). Note that a similar splitting of the spectral lines which depends on the light polarisation was observed also in the PC spectra of a ZnO single crystal.

From figure 3, it can be seen that there is a maximum in the spectrum at 370 nm and a photosensitivity drop at 378 nm for an external bias of 0.5 V (curve A), which corresponds to a small band bending. The photosensitivity drop corresponds to an energy of 3.28 eV, which is considerably lower (about 90 meV) than the ZnO band gap. A decrease in the negative bias, i.e. an increase in the band bending at the semiconductor surface, leads to the production of a maximum instead of the previously observed minimum. The photocurrent spectrum is now as figure 3, curve C, which is already at a zero external bias. Overlapping of this line with the region of bulk exciton absorption is caused by the further increase in band bending. This leads to the formation of a rather wide line with a maximum shifted towards longer wavelengths relative to the bulk exciton line (curve D).

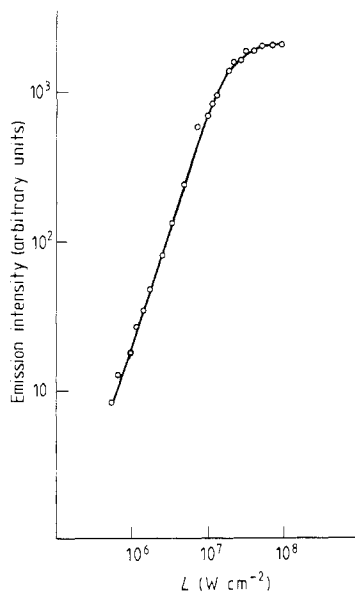


**Figure 4.** The PL intensity plotted against the optical pumping power ( $T = 78$  K).

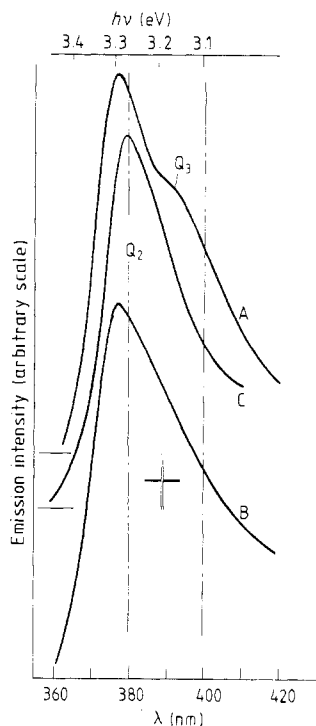


**Figure 5.** The PL spectra of ZnO in contact with an electrolyte at various external biases  $V_{ex}$  at  $T = 300$  K: curve A,  $V_{ex} = -0.5$  V; curve B,  $V_{ex} = 0$  V; curve C,  $V_{ex} = 3$  V.

## 1.3. Photoluminescence

In spite of the large number of papers concerning the luminescent properties of ZnO, the physical picture of radiative transitions near the fundamental edge is not completely understood so far and is sometimes inconsistent. Taking into account the results obtained in § 1.2, we paid special attention to such parameters as the surface potential and the optical excitation level. We succeeded in obtaining, as well as the well known line  $Q_1$  [5], the emission lines  $Q_2$  and  $Q_3$  at a low level of optical pumping and at low temperatures. The intensities of  $Q_2$  and  $Q_3$ , unlike the intensity of  $Q_1$ , essentially depend on the condition of the surface. We should point out that the dependences of the intensities  $I$  of these lines on the optical pumping power  $L$  (figure 4) were governed by a superlinear law  $I = L^n$  (where  $n = 1.6$ ) and were saturated at  $L \geq 10^7 \text{ W cm}^{-2}$ . A change in the condition of the surface over a wide range was realised by varying the ZnO crystal surface potential. To do this, the sample was immersed in an electrolyte, where the PL spectra were measured. The results of these experiments are presented in figure 5. The line  $Q_3$  was quenched (curve C) at anode biases up to about  $V_{\text{ext}} = 3.0 \text{ V}$ , i.e. with an increasing surface potential. The application of small cathode biases (a decrease in the surface potential) leads to disappearance of the line  $Q_3$  (curve C).

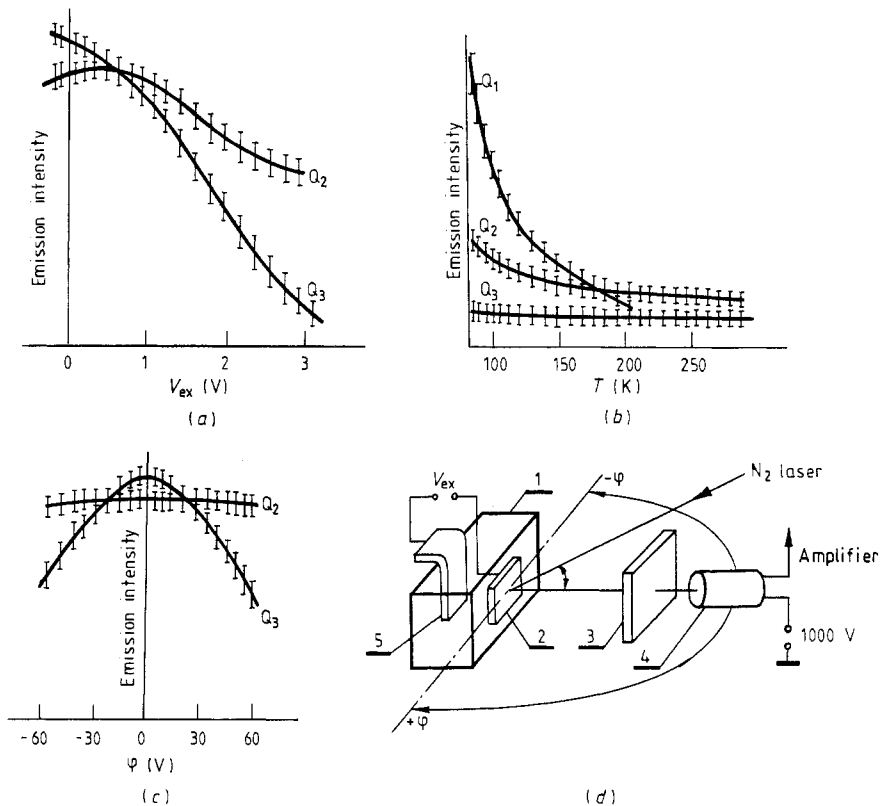


**Figure 6.** The (a) field and (b) temperature dependences and (c) direction diagrams of the emission intensities of the  $Q_2$  and  $Q_3$  lines. (d) Experimental set-up for direction diagram measurements: 1, photo-electrochemical cell; 2, sample under investigation; 3, light filter; 4, photo-electrical multiplier; 5, counter-electrode.

Some shift in the line  $Q_2$  towards a longer-wavelength region was observed, when the surface potential is increased. One can see from the field dependences of the emission intensity of  $Q_2$  and  $Q_3$  lines (figure 6(a)) that an increase in the external bias leads to the quenching of both lines. However, if the intensity of the  $Q_2$  line does not depend strongly on the surface potential, the intensity of the  $Q_3$  line sharply decreases with increase in the anode bias.

Various dependences of the intensity of either the  $Q_2$  or the  $Q_3$  line on the electric field allow us to investigate the direction diagram of emission lines. We used the set-up in figure 6(d). When an anode bias is applied to the semiconductor electrode (the  $Q_2$  line dominates in the PL spectrum (see figure 5, curve C)), the PL intensity is almost independent of the angle  $\varphi$ , which indicates the position of the photomultiplier which records the emission (figure 6(d)). This means that the PL intensity of the line  $Q_2$  is about the same for all directions, i.e. the distribution of emission is almost spherical. The dependence of the emission intensity on the angle is marked at low cathode biases when the  $Q_3$  line is pronounced in the PL spectrum.

The quenching of various luminescence lines depends on the temperature in different ways (figure 6(b)). As can be seen from figure 6, the intensity of the  $Q_2$  line decreases considerably when the temperature increases to 200 K, while that of the  $Q_3$  line remains nearly constant in the range investigated.

## 2. Discussion

On the basis of the experimental results presented in § 1, one can conclude that the above-mentioned spectral peculiarities are sensitive to the surface potential of the semiconductor and probably have similar origins. The temperature dependence of the drop in photosensitivity in the PC spectra (figure 1, curves B–D) provides sufficient evidence for us to attribute the observed peculiarities to exciton states. It is well known that absorption by bulk impurity centres is unable to change the steady photocurrent through a semiconductor–electrolyte interface significantly [4]. Also the photosensitivity drop cannot be explained by absorption on surface centres. Only exciton absorption can be the reason for such a drop in the PC spectra and interfacial photocurrent spectra (figure 3), because free-charge-carrier generation does not take place. The exciton nature of the lines in the region  $h\nu < E_g$  also follows because saturation of the emission intensity occurs at rather high powers of optical pumping (figure 4). However, attention should be drawn to the fact that the energy location of the observed lines is considerably shifted towards lower energies compared with that of bulk excitons. However, the high sensitivity to both the condition of the surface and the changes in the surface potential (see figures 2 and 3) is evidence of the surface nature of these exciton lines.

The above suggestion is confirmed by the results of an investigation into the angular dependence of emission lines. According to this dependence and taking into account the strong directivity of the  $Q_3$  emission line, one can assume that its origin in the dissociation of excitons is localised to just at the crystal surface. In fact, since the dipole moments of two-dimensional excitons are directed strictly along the surface, one could expect a more oriented characteristic, just as has been observed experimentally (figure 6(c)). The possibility of surface exciton formation connected with two-dimensional surface sub-bands of donor and acceptor type has been shown previously [6, 7]. Two-dimensional surface excitons responsible for the strongly directed  $Q_3$  emission line

(figures 5 and 6) are formed probably as a result of the Coulomb interaction between electrons and holes from the corresponding two-dimensional surface sub-bands.

Recently, [8] the reflection and electroreflection spectra of ZnO crystals were analysed; a mechanism concerning the formation of surface excitons as the result of Coulomb interaction between an electron from the conduction band and a hole from the two-dimensional surface sub-band was proposed. In this case the emission of such a quasi-two-dimensional surface exciton does not have a sharply oriented diagram; it depends strongly on the surface potential. Since the emission line satisfies the above-mentioned conditions, it may be assumed that it is due to the described types of exciton state. Note that surface excitons with this origin must play an essential role in PC and, in particular, the photocurrent through the ZnO–electrolyte interface. The spectral position of the peculiarities which they create must vary considerably depending on the location of the surface two-dimensional sub-band. Actually, as can be seen from the analysis of the experimental results, a remarkable change in the energy position of the line (from  $\lambda \approx 378$  nm to  $\lambda \approx 386$  nm) connected with the quasi-two-dimensional exciton was observed.

The analysis of the temperature dependence of the  $Q_1$ ,  $Q_2$  and  $Q_3$  line intensities (figure 6(b)) shows that the binding energies of quasi-two-dimensional and, in particular, two-dimensional exciton states considerably exceed those of bulk excitons. On the basis of this, we can estimate the critical field necessary to dissociate the bulk and quasi-two-dimensional surface excitons according to the formula  $E_{cr} = \varepsilon_{ex}/er_{ex}$  [5] ( $\varepsilon_{ex}$  and  $r_{ex}$  are the binding energy and the radius of the exciton, respectively) (note that, for surface excitons,  $\varepsilon_{ex} = R_{ex}/(n + \frac{1}{2})^2$  where  $n = 0, 1, 2$ ); we obtain  $-3 \times 10^5$  V cm $^{-1}$  and  $5 \times 10^5$  V cm $^{-1}$ , respectively.

Assuming the field strength in the space-charge region to be fixed, we can estimate its thickness from

$$W = (2\varepsilon\varepsilon_0 \Delta\varphi/eN_D)^{1/2}$$

where  $N_D$  is the concentration of ionised donors determined from the Mott–Schottky dependence according to

$$N_D = 2c^2(\Delta\varphi - kT/e)/\varepsilon\varepsilon_0e$$

where  $\Delta\varphi$  is the surface potential,  $\varepsilon$  the relative permittivity and  $C$  the capacitance.

For the external bias values used above, the mean-field intensity  $E_a$  in the space-charge region is varied in the range  $(2-8) \times 10^5$  V cm $^{-1}$ . This is found to be in good agreement with the field intensities critical for exciton dissociation obtained above.

Thus, when the field increases (figure 3, curves B–D), dissociation of surface excitons is initiated, i.e. additional charge carriers are created, the previously observed drop is transformed into a maximum and overlap with the bulk exciton line occurs.

Attention should be also drawn to the correlation between the PL and photocurrent spectra when the exciton field dissociation takes place. In fact, if the surface field increases, a transformation of the photocurrent minimum into a maximum as a result of field dissociation of quasi-two-dimensional excitons occurs (figure 3) while, at the same field, quenching of the corresponding line of surface exciton luminescence is observed (figure 6(a)).

It is important to note from the viewpoint of solar energy photo-electrochemical conversion that the smooth variation in surface potential over a large range in such systems allows us to control the degree of field dissociation of both bulk and quasi-



two-dimensional excitons and to broaden the spectral region of photosensitivity, thus increasing the conversion efficiency.

### 3. Conclusion

At present, there are other models which also describe the spectra of excited states at the solid surface [5, 9, 10], apart from those mentioned above. However, in the surface exciton model, either only one of the charge carriers is bound to the surface or the strict two-dimensionality is a theoretical approximation for large anisotropy of the effective mass tensor ( $m_z \gg m_x, m_y$ ), while the weakening of this inequality (which occurs in a real situation) leads to simple localisation in the surface layer.

In other models in which surface excitons are considered to be localised in the same surface layer [11] and differ from the bulk excitons because of the presence of an electric field, there is also no reason to assume that they are strictly oriented. However, the strongly directed emission of the observed line confirms the possibility of two-dimensional exciton formation [6, 7]. This also confirms the model of surface excitons connected with two-dimensional surface sub-bands with wavefunctions which decay over distances equal to two or three times the lattice constant.

The mechanism of quasi-two-dimensional excitons [8] connected with one definite two-dimensional surface sub-band is also of interest. Such excitons can differ from two-dimensional excitons.

### References

- [1] Kusmina I P and Nikitenko V A 1984 *Zinc Oxide. Preparation and Optical Properties* (Moscow: Nauka) (in Russian)
- [2] Harutunian V M, Sarkisian A G, Panossian J R, Akopian R S, Arakelian A O and Margarian A L 1980 *Izv. Acad. Nauk Arm. SSR, Phys.* **15** 438 (in Russian)
- [3] Kolb D M and Schulz H I 1981 *Springer Current Topics in Materials Science* vol 7 (Berlin: Springer) p 227
- [4] Panossian J R, Harutunian V M, Sarkisian A G, Meliksetian V A, Margarian A L and Stepanian G M 1982 *Sov. Phys.-Semicond.* **16** 832
- [5] Litovchenko V G 1980 *Fundamentals of the Physics of Sliding Semiconducting Systems* (Kiev: Naukova Dumka) (in Russian)
- [6] Ginsburg Y L and Kelle V V 1973 *Zh. Eksp. Teor. Fiz. Pis. Red.* **17** 428
- [7] Bobrysheva A I, Beryl S I, Zyukov V I, Moskalenko S A and Pokatylov E P 1983 *Phys. Status Solidi* **b** **115** 153
- [8] Panossian J R, Kasamian Z A and Mailian A R 1985 *JETP Lett.* **41** 307–10
- [9] Lozovic Yu E and Nishanov V N 1976 *Sov. Phys.-Solid State* **18** 3267
- [10] Agranovich V M, Lozovic Yu E and Malschikov A G 1975 *Sov. Phys.-Usp.* **18** 925
- [11] Kiselev V A 1978 *Sov. Phys.-Solid State* **20** 2173